

Ring cavity surface emitting quantum cascade laser with a near Gaussian beam profile

Pedro N. Figueiredo*, Andrey Muraviev, Robert E. Peale

Physics Department, University of Central Florida, Orlando, FL, USA 32816

ABSTRACT

We propose a vertical spiral phase corrector for ring cavity surface emitting (RCSE) quantum cascade lasers (QCLs), which will allow achievement of near-Gaussian generated beam profile. A problem with RCSE QCLs is their donut-shaped intensity distribution with a node along the symmetry axis of the ring. This arises because of the π phase difference for the azimuthally polarized rays emitted from opposite elements of the ring. We theoretically demonstrate that near-Gaussian beams can be achieved with a spiral phase shifter that adds one wavelength of additional optical path in going once around the ring. Various three dimensional lithographic techniques for fabricating such a phase shifter, including a grey scale mask, electron-beam resist dose dependency, and two photon induced photopolymerization, are considered. Ring cavity QCLs with the proposed phase corrector will feature better beam quality, larger power, and better resistance to radiative damage in comparison with traditional edge-emitting QCLs.

Keywords: Ring cavity, quantum cascade laser, beam quality, surface emission

1. INTRODUCTION

The quantum cascade laser (QCL) is a unipolar device in which individual electrons undergo multiple photon emissions via transitions between states in a periodic sequence of quantum wells.¹⁻⁷ The QCL emission wavelength is determined by quantum well design. Most commercial QCLs emit from their end facets with strongly diverging beams due to the small exit apertures. Experimental ring-cavity surface emitting QCLs achieve better beam quality due to larger and symmetric exit apertures. Output coupling is usually achieved via a 2nd-order distributed-feedback grating. Emission from opposite sides of the ring is 180 degrees out of phase, causing destructive interference along the axis of symmetry, resulting in a donut-shaped intensity profile.

Additional azimuthal oscillations in the intensity profile⁸ are caused by beating between the grating period and emission wavelength. The solution is already known, namely to match the grating to the wavelength. This usually requires fabricating many devices with different grating periods, and choosing the one with the fewest azimuthal hot spots.

In this paper, we propose a means of eliminating the most significant of the beam profile problems for RCSE QCL, namely the central node. Our approach shifts the phase of the emission by use of a vertical spiral wedge of dielectric. Such a wedge may be fabricated by a number of different three dimensional lithography methods.

2. THEORETICAL CONSIDERATIONS

Figure 1 (left) presents a schematic of the coordinate system and geometrical parameters. Laser radiation is emitted in the z direction from the top facet of the ring. Huygens principle gives for any field component u_p at the observation point P,⁹

$$u_p = \int \frac{kue^{ikR}}{2iR\pi} df_n \quad (1)$$

*figueiredo.p.n@knights.ucf.edu;

where k is the wavevector magnitude, R is the distance from area element $d\mathbf{f}$ to P, and u is the field value at $d\mathbf{f}$. The integral is performed over the emitting surface, i.e. the top surface of the ring, and df_n is the projection of the surface area element $d\mathbf{f}$ on the direction of the ray from the light source within the ring to $d\mathbf{f}$. The area element $d\mathbf{f}$ is already in the same direction as the assumed direction vector \mathbf{n} (z direction) of the rays from the source of emission within the ring to the exit aperture on the top surface of the ring, so that $df_n = df = wad\phi$, where w is the width of the ring waveguide. Without loss of generality, given the azimuthal symmetry, we may align the coordinates so that the x -axis is directly under the field point P, so that only the polar angle (Θ_0) and field point radius vector (R_0) are needed to specify the position of P. The polar angle for the position of each area element is $\pi/2$, so that only the azimuthal angle ϕ and ring radius a are necessary to specify an area element's position. With these coordinates, the vector from area element to field point P is $\mathbf{R} = \mathbf{R}_0 - \mathbf{a} = \{R_0 \sin \Theta_0 - a \cos \phi, -a \sin \phi, R_0 \cos \Theta_0\}$.

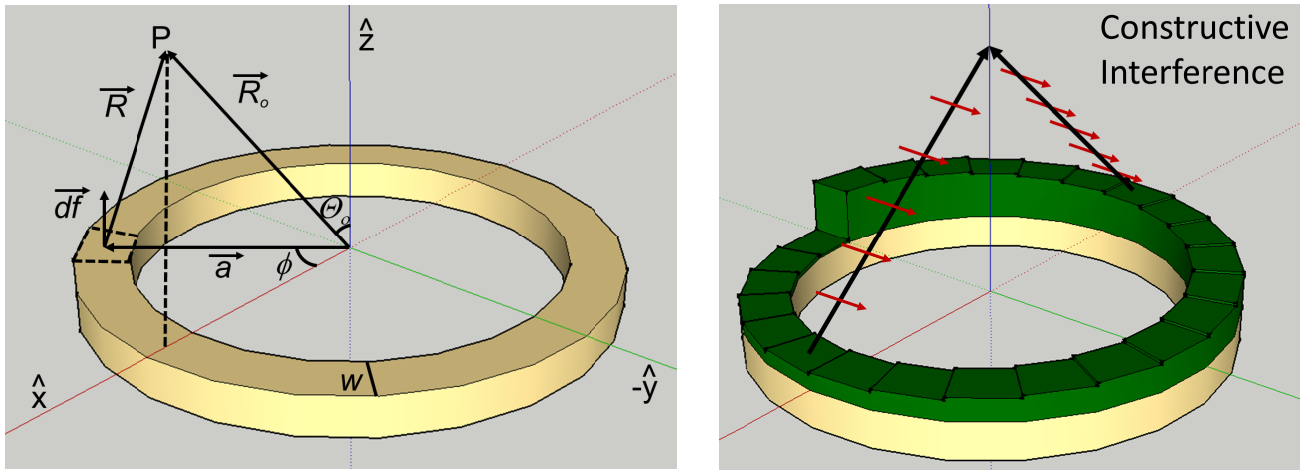


Figure 1. (left) Geometry for calculation of ring-cavity emission profile. Field point P lies above the x axis. (right) Proposed spiral wedge phase shifter giving constructive interference along the symmetry axis for beams from opposite sides of the ring.

Since $a \ll R_0$, $R = \sqrt{(R_0^2 + a^2 + 2R_0a \sin \Theta_0 \cos \phi)} \approx R_0 - a \sin \Theta_0 \cos \phi$. Since the range of Θ_0 is small, keeping the angle dependent terms in the denominator of Eq. (1) gives only slow variations with polar angle, so there we take $R \approx R_0$. On the other hand the factor ka in the argument of the complex exponential may be large, giving rise to a large phase that oscillates rapidly with small changes in polar angle, so there we must keep the second term in the expansion of R . Then, Eq. (1) becomes

$$u_p = \frac{wake^{ikR_0}}{2i\pi R_0} \int_0^{2\pi} ue^{-ika \sin \Theta_0 \cos \phi} d\phi \quad (2)$$

The azimuthally-polarized¹⁰ electric field of the emitted wave at the surface of the ring is $\mathbf{E} = E_0\{-\sin \phi, \cos \phi, 0\}$. We may then write

$$E_{py} - iE_{px} = \frac{wake^{ikR_0}}{2i\pi R_0} E_0 \int_0^{2\pi} e^{-ika \sin \Theta_0 \cos \phi} e^{i\phi} d\phi \quad (3)$$

E_{px} calculates to zero because contributions from members of each pair of opposite area elements equally distant from P have opposite sign, and their contributions cancel. However, opposite area elements that have equal but opposite y components are at different distances from P and do not completely cancel. The Bessel function in integral form is¹¹

$$J_n(z) = \frac{1}{2i^n \pi} \int_0^{2\pi} e^{iz \cos \phi} e^{in\phi} d\phi \quad (4)$$

so that

$$E_{py} = -\frac{wake^{ikR_o} E_o}{R_o} J_1(ka \sin \Theta_o) \quad (5)$$

where we have used the property that J_1 is an odd function of its argument.

To eliminate the central node, a spiraling wedge is added to the output facet of the ring, such that the phase of the emitted light is shifted by 2π in going once around the ring. Such a vertical spiral wedge is depicted schematically in Fig. 1 (right). This shift is introduced as an additional angle dependence on the phase term in Eq. (1)

$$u_p = \frac{wake^{ikR_o}}{2i\pi R_o} \int_0^{2\pi} u e^{-ika \sin \Theta_o \cos \phi + i\phi} d\phi \quad (6)$$

Then

$$E_{py} - iE_{px} = -\frac{wake^{ikR_o} E_o}{iR_o} J_2(ka \sin \Theta_o) \quad (7a)$$

$$E_{py} + iE_{px} = \frac{wake^{ikR_o} E_o}{iR_o} J_0(ka \sin \Theta_o) \quad (7b)$$

where we have made use of the evenness of the functions J_0 and J_2 with respect to their arguments. Equations (7a) and (7b) give

$$E_{py} = \frac{wake^{ikR_o} E_o}{2iR_o} [J_0(ka \sin \Theta_o) - J_2(ka \sin \Theta_o)] \quad (8a)$$

$$E_{px} = -\frac{wake^{ikR_o} E_o}{2R_o} [J_0(ka \sin \Theta_o) + J_2(ka \sin \Theta_o)] \quad (8b)$$

The intensity obtained by summing the absolute squares of the fields in equations (5) and (8) are plotted as a function of polar angle Θ_o in figure 2. Results with the wedge show a central peak whereas those without have the usual a central node.¹⁰

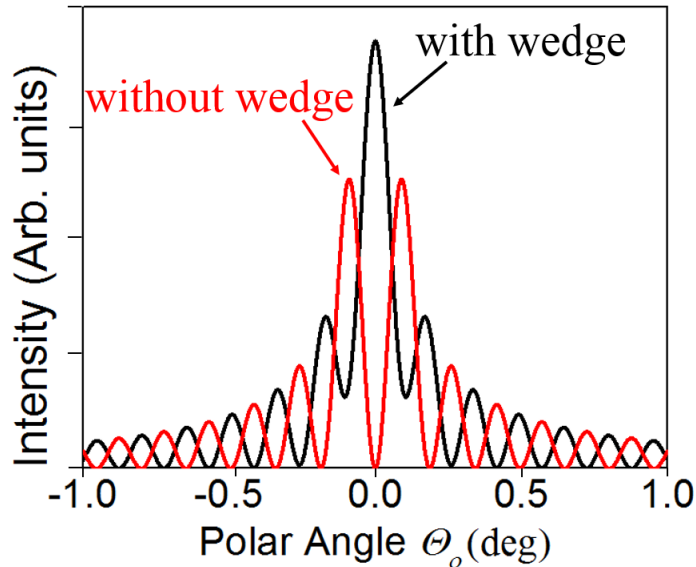


Figure 2. Intensity distribution as a function of polar angle θ_0 with and without the spiral wedge, as indicated.

3. EXPERIMENT

The considered spiral wedge may be fabricated by a three dimensional lithography such as gray scale mask,^{12,13} two-photon lithography, or electron-beam lithography. We used the latter in this initial study. A JEOL scanning electron microscope equipped with Nanometer Pattern Generation System (NPGS) patterned a design in discretized areas using different electron doses. Then we timed the development according to the dependence of development rate on dose. The result is presented in figure 3 C. We then transferred the spiral wedge pattern into the silicon substrate by reactive ion etching (Trion MiniLock II). By controlling the gas chemistry, we control the removal rate of the polymer mask, and thus etch the wedge into the substrate.

Specific key process parameters of the entire process are:

- 1) Spin on 495 PMMA A15 on virgin grade Silicon wafer @ 2000 RPM and bake solvent
- 2) Spiral dose exposure using NPGS
- 3) Timed 30s development in 1:3 methyl isobutyl ketone (MIBK) : isopropyl alcohol (IPA)
- 4) ICP RIE RF plasma – 300 W ICP, 200 W RIE, 40 sccm SF₆, 5 sccm O₂, 10 minutes
- 5) RIE RF plasma – 100 W RIE, 50 sccm O₂, 2 minutes

Figure 3A presents an optical microscope image of the wedge, and Figure 3B presents the line profile across the wedge. The depth difference between opposite sides is ~350 nm so that the total height of the wedge that has been etched into silicon is $d = 700$ nm. The phase difference for two waves from opposite sides of the ring with an ideal wedge is $\pi(n-1)d/\lambda$. We consider the height for a wedge etched into the InP substrate of a substrate-emitting RCSE QCL. For the desired phase difference of π , an index of 3.1 for InP, and a wavelength of 5 μm , the desired wedge height would be 2.4 μm . With optimization of the differential etch rate for mask and wedge material, the desired wedge seems feasible.

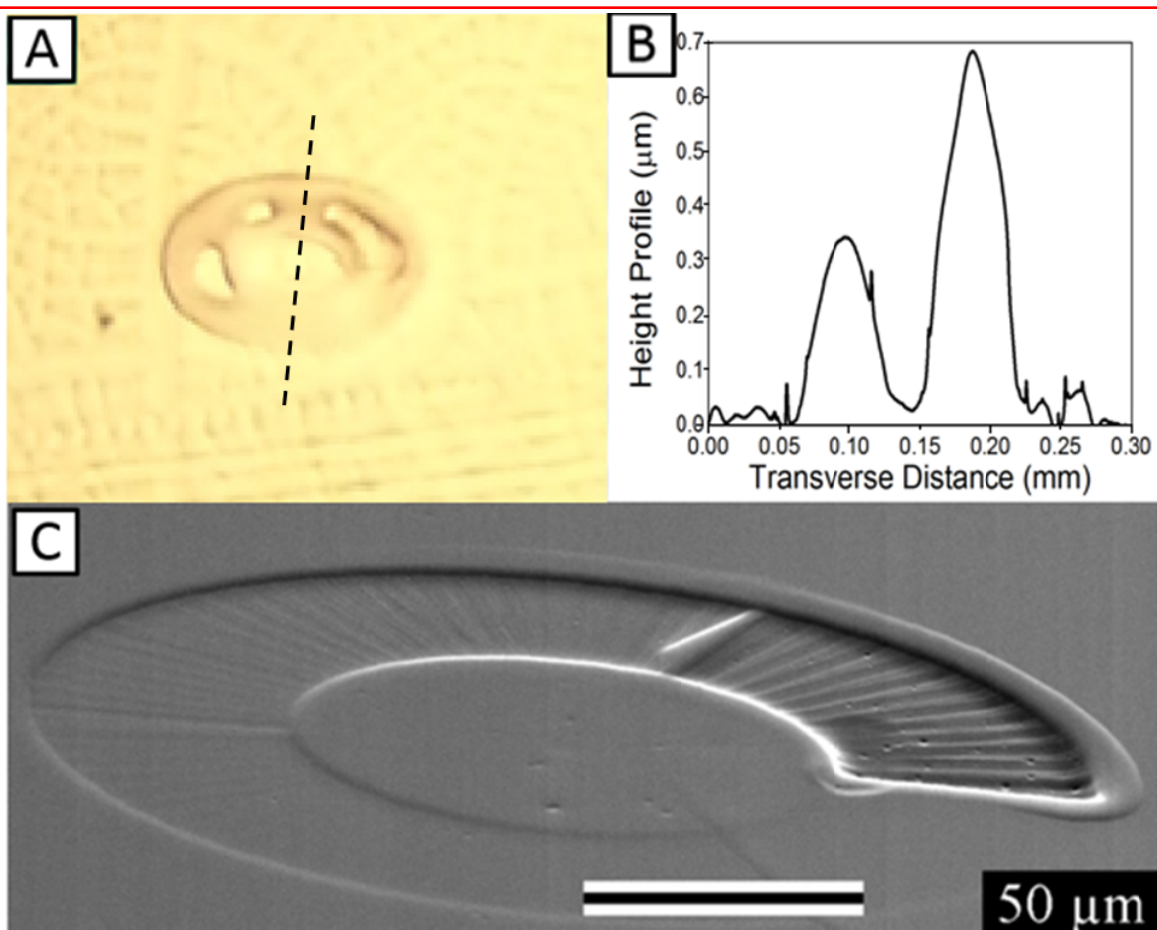


Figure 3. (A) Optical image of a 300µm spiral ring fabricated into silicon. The dashed line indicates the profilometer track. (B) Height profile across along the spiral diameter. (C) Angled Scanning Electron Microscope image of the spiral written in e-beam resist.

Electron beam lithography is slow and inappropriate for large area patterning. For wafer scale fabrication, a grey scale photolithographic mask is more desirable. Such may be prepared using high energy beam sensitive glass (HEBS). The HEBS material's transmittance is a function of an electron beam exposure time. The HEBS mask with the ring patterns variable opacity may be used repeatedly in standard photolithography. Wedges in photoresist are then created according to the dependence of development rate on UV exposure. Resist wedges may then serve as etch masks¹³.

We may also fabricate the spiral by use of a direct laser writer (DLW), i.e. a two photon lithographic system. A spiral may be formed by direct exposure and a single dissolution¹⁴. An advantage over electron beam lithography is the possibility of much thicker polymers to allow for deeper spirals. A disadvantage is speed and practically limited areas of exposure.

4. SUMMARY

This paper described a means of eliminating the central node in the beam from a ring-cavity surface emitting quantum cascade laser. Proposed is a wedge of dielectric fabricated on the emitting surface of the ring, so that a phase shift of 2π is added in going once around the ring. Initial experiments in 3D lithography demonstrate the feasibility of fabricating the required wedge.

REFERENCES

- [1] Kazarinov, R., Suris, R., "Possibility of amplification of the electromagnetic waves in a semiconductor with a superlattice," *Soviet Physics Semiconductor* 5, 707-709 (1971).
- [2] Faist, J., Capasso, F., Sivco, D. L., Sirtori, C., Hutchinson, A. L., Cho A. Y., "Quantum Cascade Laser," *Science* 264, 553-556 (1994).
- [3] Paiella, R., [Intersubband Transitions in Quantum Structures], McGraw-Hill, New York NY (2006).
- [4] Evans, A., Darvish, S. R., Slivken, S., Nguyen, J., Bai, Y., Razeghi, M., "Buried heterostructure quantum cascade lasers with high continuous-wave wall plug efficiency," *Applied Physics Letters* 91, 071101 (2007).
- [5] Beck, M., Faist, J., Oesterle, U., Ilegems, M., Gini, E., Melchior, H., "Buried heterostructure quantum cascade lasers with a large optical cavity waveguide," *Photonics Technology Letters, IEEE* 12, 1450-1452 (2000).
- [6] Blaser, S., Yarekha, D., Hvozdar, L., Bonetti, Y., Muller, A., Giovannini, M., Faist, J., "Room-temperature, continuous-wave, single-mode quantum-cascade lasers at $\lambda \approx 5.4 \mu\text{m}$," *Applied Physics Letters* 86, 041109 (2005).
- [7] Bai, Y., Slivken, S., Darvish, S. R., Razeghi, M., "Room temperature continuous wave operation of quantum cascade lasers with 12.5% wall plug efficiency," *Applied Physics Letters* 93, 021103 (2008)
- [8] Mujagic, E., Nobile, M., Detz H., Schrenk, W., Chen, J., Gmachl, C., Strasser, G., "Ring cavity induced threshold reduction in single-mode surface emitting quantum cascade lasers," *Applied Physics Letters* 96, 031111 (2010).
- [9] Landau, Lifshitz, [The Classical Theory of Fields, 4th edition], Butterworth Heinemann, Amsterdam (1975).
- [10] Bai, Y., Tsao, S., Bandyopadhyay, N., Slivken, S., Lu, Q. Y., Caffey, D., Pushkarsky, M., Day, T., Razeghi, M., "High power, continuous wave, quantum cascade ring laser," *Applied Physics Letters* 99, 261104 (2011).
- [11] Weisstein, E. W., "Bessel Function of the First Kind." From MathWorld--A Wolfram Web Resource. <http://mathworld.wolfram.com/BesselFunctionoftheFirstKind.html>
- [12] Chang, D. H., Azfar, T., Kim, S. K., Fetterman, H. R., Zhang, C., Steier, W. H., "Vertical adiabatic transition between a silica planar waveguide and an electro-optic polymer fabricated with gray-scale lithography," *Optics letters* 28, 869-871 (2003).
- [13] Gimkiewicz, C., Hagedorn, D., Jahns, J., Kley, E.-B., Thoma, F., "Fabrication of microprisms for planar optical interconnections by use of analog gray-scale lithography with high-energy-beam-sensitive glass," *Applied optics* 38, 2986-2990 (1999).
- [14] Nawrot, M., Nawrot, Zinkiewicz, L., Włodarczyk, B., Wasylczyk, P., "Transmission phase gratings fabricated with direct laser writing as color filters in the visible," *Optics Express* 21, 31919 (2013).